Published in final edited form as:
Am J Geriatr Psychiatry. 2009 January ; 17(1): 30–42. doi:10.1097/JGP.0b013e31817b60af.

Altered Functioning of The Executive Control Circuit in Late-Life Depression: Episodic and Persistent Phenomena

Howard J. Aizenstein, MD, PhD[a,b], **Meryl A. Butters, PhD**[a], **Minjie Wu, MS**[c], **Laura M. Mazurkewicz, BS**[a], **V. Andrew Stenger, PhD**[d], **Peter J. Gianaros, PhD**[a], **James T. Becker, PhD**[a], **Charles F. Reynolds III, MD**[a], and **Cameron S. Carter, MD**[e]

a *Department of Psychiatry, University of Pittsburgh, Pittsburgh, PA 15213*

b *Department of Bioengineering, University of Pittsburgh, Pittsburgh, PA 15213*

c *Department of Electrical & Computer Engineering, University of Pittsburgh, Pittsburgh, PA 15213*

d *Department of Medicine, University of Hawaii at Manoa School of Medicine, Honolulu, HI 96813*

e *Department of Psychiatry, University of California at Davis, Sacramento, CA 95817*

Abstract

Objective—To characterize the functional neuroanatomy of late-life depression (LLD) by probing for both episodic and persistent alterations in the executive-control circuit of elderly adults.

Design—Event-related fMRI data were collected while participants performed an executive-control task.

Setting—Participants were recruited through a depression-treatment study within the Pittsburgh Intervention Research Center for Late-Life Mood Disorders.

Participants—13 non-depressed elderly comparison participants and 13 LLD patients.

Intervention—The depressed patients underwent imaging before initiating and after completing 12 weeks of paroxetine.

Measurements—Regional fMRI activity was assessed in the dorsolateral prefrontal cortex (dLPFC: BA9 and BA46 bilaterally) and the dorsal anterior cingulate cortex (dACC). Functional connectivity was assessed by correlating the fMRI time-series in the dLPFC and dACC.

Results—Both depressed and comparison participants performed the task as expected, with greater response latency during high versus low-load trials. The response-latency load-effect did not differ between groups. In contrast to the null findings for behavioral data, pre-treatment, depressed patients showed diminished activity in the dLPFC (BA46 left, $t(25)=1.9$, $p=.035$) and diminished functional connectivity between the dLPFC and dACC. Moreover, right dLPFC (BA46 right, $t(25)=2.17$, $p<.02$) showed increased activity after treatment.

Conclusions—These results support a model of both episodic and persistent neurobiologic components of LLD. The altered functional connectivity, perhaps due to vascular damage to frontal white matter, appears to be persistent. Further, at least some of the pre-frontal hypoactivity (in the right dLPFC) appears to be an episodic characteristic of acute depression amenable to treatment.

Correspondence to: Howard J. Aizenstein.

Corresponding Author: **Howard J. Aizenstein, M.D., Ph.D.** Departments of Psychiatry and Bioengineering Western Psychiatric Institute and Clinic 3811 O'Hara Street Pittsburgh, PA 15213 Phone: 412-383-5452 Fax: 412-383-5458 Email: aizen@pitt.edu.

Keywords

fMRI; Geriatric depression; Cognitive control

Introduction

Depression in the elderly is common and causes significant distress and disability. Approximately 15% of the elderly have significant depressive symptoms (1). Depression is the second leading cause of 'global disease burden' (2), the leading predictor of poor outcome from medical illnesses such as heart disease (3,4), and the primary diagnosis in most elderly suicides (5). Moreover, the number of elderly is expected to double by 2030 (6), further increasing the public health burden of late-life depression (LLD). Unfortunately, current depression treatments, which are borrowed from the treatment of mid-life depression, are only partly effective in the elderly; 40-50% of those with LLD have a delayed or limited response to first-line antidepressant treatment (7). Much of the limited response may be due to differences in the underlying neurobiology between mid-life depression and LLD. However, the neurobiologic bases of the depressive syndrome and treatment response in LLD are not well understood.

A prominent theory for delayed or brittle response in LLD is that the neuropathology in LLD is distinguished by cerebrovascular and/or neurodegenerative changes, which are associated with dysfunction in frontostriatal cognitive circuits. Convergent evidence from structural MRI, cognitive assessment, and electrophysiologic studies supports the frontostriatal hypothesis of LLD (8). Conventional structural MRI, Diffusion Tensor Imaging (DTI), and Magnetic Resonance Spectroscopy (MRS) studies (9-13) have shown that elderly depressed individuals have higher rates (compared to age-matched non-depressed individuals) of gray and white-matter brain structural changes affecting frontal and subcortical areas, and consistent with small vessel ischemic disease. Cognitive assessment in LLD shows a pattern of impairment in executive tasks and slowed information processing speed, also suggestive of dysfunction of frontal and striatal cognitive circuits (14). Functional neuroimaging studies in LLD have shown decreased resting cerebral blood flow and glucose metabolism in prefrontal and anterior cingulate regions of the brain (15). Additionally, we have recently shown altered functioning in the dorsolateral prefrontal cortex (dLPFC) and striatum in LLD during a sequence learning task (16). Similar findings of decreased dLPFC and dACC activation have also been found in mid-life major depression (17).

Among the particular cognitive functions subserved by the frontostriatal circuit are those that are often described as executive or cognitive control. In fact, there seem to be several discrete components of executive-control, which can be mapped to different anatomic regions of the prefrontal cortex. For instance, MacDonald et al (18) illustrated the different roles of the dLPFC and dACC during a cognitive-control task. In MacDonald's study, comparison subjects performed a Stroop task in which each trial was preceded by an instruction, either 'read the word' or 'name the color'. This was followed by a delay and then the Stroop stimulus. The dLPFC was active during the instruction phase, showing heightened activity with increased preparatory demand (i.e., the color naming instruction), whereas, the dACC was selectively active during the response phase, also showing heightened activity on the color naming trials, which are associated with high response conflict.

The current study was designed to examine the dLPFC - dACC cognitive-control circuit in LLD. To the extent that LLD is associated with frontostriatal dysfunction, we hypothesized that we would detect alterations in activation during a Stroop task. Specifically, following from previous PET and fMRI studies (15), we expected decreased dLPFC and dACC activation in

LLD, and due to the evidence of prefrontal white matter damage in LLD, we also expected decreased functional connectivity (evaluated with dLPFC to dACC time-series correlations) in the depressed subjects compared to non-depressed comparison subjects.

In this study we specifically questioned how the changes in functional activation are affected by treatment and response: Are changes in the circuit's function limited to or specific to the acute depressed episode, or do they persist once patients respond to treatment? If they persist do they reflect the underlying persistent neurobiology, i.e., the biological changes that make someone vulnerable to depression? Since the structural white matter changes are persistent, we predicted that changes in functional connectivity would persist despite treatment and response. However, the decreased regional dLPFC and dACC activation might resolve with treatment response, as has previously been shown for mid-life depression (19).

Methods

Research Participants

Thirty participants completed MR scanning for this study. However, data from three (one depressed and two comparison participants) were unusable due to computer malfunction, and evidence of a subcortical stroke was identified during the structural scan on one additional comparison participant. Data from the remaining twenty-six participants were analyzed. These included 13 elderly comparison participants and 13 patients with LLD. All underwent a SCID-IV evaluation, which was used to establish the diagnosis of a current Major Depressive Episode (non-psychotic and non-bipolar) and the age of first lifetime depression. Other than MDD (for participants comprising the depressed group) and the anxiety disorders, all other Axis I disorders were used as exclusion criteria. Participants were also excluded for a history of stroke or significant head injury, Alzheimer's, Parkinson's, or Huntington's disease. We chose to include those with anxiety disorders due to the high prevalence (48%) of anxiety disorders in individuals with LLD (20). Five of the 13 LLD participants and 2 of the 13 comparison participants met criteria for an anxiety disorder. In almost all cases the anxiety disorder was generalized anxiety disorder, but there were also individual cases of specific phobia, post-traumatic stress disorder, social phobia, and anxiety disorder NOS. Participants were excluded if they had taken psychotropic medications during the 2 weeks prior to imaging. Medications other than anti-depressants were acceptable, as medication use is common in the elderly population. Medication use was distributed similarly between the depressed and comparison participants.

All depressed participants had late-onset LLD, with their first episode of depression starting after the age of 50. All subjects were right-handed. Demographics of the sample are shown in Table I.

Participants were recruited through the University of Pittsburgh's Intervention Research Center for Late-Life Mood Disorders (IRC/LLMD). The depressed participants were recruited from an ongoing open-label treatment study of paroxetine for major depression (21). Depressed participants underwent fMRI scanning before starting anti-depressant medication. The mean Mini Mental State Exam (22) score for the elderly comparison participants and depressed participants was not different, ($t(24)=1.20$, $p=.25$). Informed consent was obtained prior to scanning through procedures approved by the University of Pittsburgh's Institutional Review Board. Each participant was paid $50.

Procedures

Preparing to Overcome Prepotency (POP) task

Participants were trained on the task outside the MR scanner for as long as needed to familiarize them with the task (5-10 minutes). The task (which we refer to as the POP task) is specific for the dLPFC and dACC cognitive-control circuit. It is derived from the switching Stroop task, MacDonald et al (18). This task has two components, separated by a delay: an instruction (or cue) phase and a decision (or probe) phase. As in the switching Stroop task, the instruction (cue) phase involves an executive maintenance component meant to engage the dLPFC and a decision (i.e., conflict monitoring) phase meant to engage the dACC.

The POP task (Figure 1) involves presentation of cues (green/red square) during the preparation phase of the task, indicating whether response to an upcoming probe (arrow on right/left) should be congruent (low-load condition) or incongruent (high-load condition). During congruent conditions, the participant has to push a button underneath the left index finger if the arrow is pointing left, while s/he has to push a button placed underneath the right index finger if the arrow is pointing right. During incongruent tasks, the participant has to invert this order (e.g. push the button underneath her or his left index if the arrow is pointing right). Red and green cues alternated quasi-randomly during the task and 25% of the trials contained a red cue. Indicators of behavioral performance included accuracy rates (number of correct answers / number of total answers), reaction time (RT, msec) calculated on correct trials only, and percent increase in RT ([average RT in high-load minus average RT in low-load conditions] / average RT in low-load conditions). The percent increase in RT was considered a measure of the load-effect, in that it indicated a proportionally slower response during high-load compared to low-load tasks.

Scanning Procedures

Data Acquisition

Imaging data were collected with a 1.5T Signa scanner (GE Medical Systems). High-resolution anatomical images (SPGRs) were acquired for each participant. Additionally, T1-weighted structural images were acquired with a 3.8 mm thickness (in-plane with the functional images). These had 36 oblique-axial slices oriented parallel to a line from the anterior to posterior commissures (the AC-PC line), with an in-plane resolution of 0.9375 mm × 0.9375mm and with a field of view of 240mm. Functional images were acquired using a one-shot spiral sequence with TE=35ms and TR=2000ms; 26 oblique-axial slices were acquired with an in-plane resolution of 64×64 with 3.75mm × 3.75mm and a slice thickness of 3.8 mm, with a field of view of 240 mm.

Images were acquired in four blocks of 24 trials each. There were 10 scans per trial. Each trial lasted 20 seconds. The cue was presented for 0.5 seconds, followed by 9.5 seconds of a fixation cross in the center of the screen. The probe was then presented for 0.5 seconds, followed by 9.5 seconds of fixation before the next cue.

Behavioral Data Analysis

The primary performance measures on the POP task were the differences in RT and accuracy between high-load and low-load trials. Within-group comparisons used within-subject, paired t-tests of RT and accuracy to test our prediction that in each group there would be significantly greater RT and significantly lower accuracy on the high-load trials versus the low-load trials. To test for differences across groups on RT and accuracy, we used an ANOVA testing the interaction of group-by-condition. To test for fatigue and learning effects we compared reaction-time and accuracy during the first 20 trials with the reaction and accuracy data during

the final 20 trials. These tests of fatigue and learning effects were done within each group using within-subject, paired t-tests.

Imaging Analysis

Data Preprocessing

Motion correction was performed using a 6-parameter linear algorithm (23). A linear detrending algorithm was also performed, using only data within 3 standard deviations of the mean to estimate the linear trend. An outlier correction algorithm was performed to remove data that was more than 7 standard deviations from the mean. Outlier correction was used primarily to remove voxels that had signal drop-out (primarily due to movement that would move a voxel into CSF or out of brain), and thus led to a very large deviation from the mean (thus 7 SD was sufficient for these extreme outliers). To remove less extreme outliers we relied on our procedure of only choosing the single voxel with the most significant main effect of trial, which excludes all other voxels with high variance. Global normalization was performed multiplicatively to give each subject a mean intensity of 3000. All analyses were conducted on a single-subject basis on non-cross-registered data. The ROIs were defined using the Automated Labeling Pathway (described below), the extracted ROI data were analyzed using MATLAB (Mathworks, Natick, MA). The statistical analyses were done in JMP 5.0 (SAS Institute, Cary, NC).

The anatomical ROIs were chosen based on our previous fMRI studies of cognitive control (e.g., studies employing the Switching Stroop Task (18) and the POP task (24,25)). The specific regions chosen were the dLPFC (BA9 and BA46 bilaterally), defined in the Brodmann area map obtained from the MRIcro software package (26) and the dACC (which spanned a central portion of both right and left BA32) chosen from a previous functional imaging study (27).

Automated Labeling Pathway

In order to define each ROI for subject in his/her own space, we used an automated labeling pathway, which has been previously validated for fMRI (28). This involved registering the Montreal Neurological Institute (MNI) Colin27 brain to each subject's SPGR using a fully-deformable registration implemented in ITK (Insight Segmentation and Registration Toolkit (29)). Each ROI was then transformed into each subject's anatomic space using the deformable transformation. A gray matter mask was applied to each ROI, using the FAST algorithm (30). The labeling of each subject's ROIs was visually inspected to assure accurate mappings.

Time-Series Analysis

For each participant and each ROI, time-series were generated for both high-load and low-load correct trials. Trials in which participants made errors or failed to respond were excluded from the analysis. In this way, differences in performance across groups would not be responsible for observed differences in the fMRI time-series; rather differences would reflect brain activation during similar performance. To allow for different locations of the peak of activation across participants we chose the most significant voxel for each participant for each ROI, similar to the approaches used in other fMRI studies of aging (31,32). A particular advantage of this approach (i.e., choosing the most significant voxel on an individual basis) is that this allows for variability of location and peak of hemodynamic response across participants who differ in sulcal and gyral anatomy. Additionally, choosing a small peak region on an individual basis appears to be less susceptible to age-related differences in the BOLD HRF (33). A noted limitation of this approach, however, is that it only examines the peak of activity and ignores the spread, or size of activity. For the dLPFC the most significant voxel was chosen as the voxel that correlated most strongly with a standard hemodynamic response function (HRF, (34)) convolved with cue-onset, thus focusing on the maintenance role ascribed to the dLPFC.

For the dACC the most significant voxel was chosen as the voxel that correlated most strongly with the standard HRF convolved with probe onset, thus focusing on the dACC conflict-monitoring phase of the task.

As in previous studies using this and similar tasks (18,24,25), resulting time-series values were transformed into a percent change from baseline, with scan 1 used as the baseline for dLPFC (i.e., cue-related activity) and scan 10, used as the baseline for dACC (i.e., probe-related activity). A paired t-test analysis was then performed on each region comparing the mean HRF of the high-load trials versus the mean HRF of low-load trials. For the dLPFC, the mean was calculated across scans 2-5, when the cue-related activity is expected to peak (18). For the dACC, the mean was calculated across scans 6-9, when conflict-related activity is expected to peak (18). Based on previous studies with this and similar tasks, we expected greater signal for the high-load versus the low-load trials, thus one-tailed p-values are reported. Since each voxel was selected based on the maximum trial-related activity (not whether high-load or low-load) this paired t-test is orthogonal to the voxel-selection criteria and does not require additional multiple comparison correction for the number of voxels in the region. Two-sample t-tests were done to compare the signal between patients (pre- and post-treatment) and comparison participants. Paired t-tests were then used to compare depressed participants pre- and post-treatment. The comparisons between groups used the activity on the high-load trial only, the condition that was expected to have the greatest effect.

Whole Brain Voxel-wise Analysis

In addition to the primary ROI-based analyses that were done to test our specific hypotheses, we also performed an exploratory whole brain voxel-wise analysis. For this analysis, we used the same fully-deformable registration pathway used for the ROI-based analysis, but in this case we applied the registration to map each subject's fMRI data to a common space (the MNI Colin27 atlas). Prior to registering the fMRI data, the same preprocessing was done on the fMRI data, as in the ROI-based analysis - motion correction, detrending, and outlier correction. The preprocessed and aligned functional data were analyzed within each group using a 2-way ANOVA testing the effect of condition (Red vs Green) versus Scan number (1-10). This analysis was done using the NIS and Fiswidgets software package (35). The results were thresholded with a voxel-wise $p = .01$ and an 8-voxel contiguity threshold to correct for multiple comparisons. This corresponds to an image-wise false-positive rate of .01 (36).

Functional Connectivity Data Analysis

To test whether there was altered connectivity in the executive-control circuit, we examined the correlations within each participant on the fMRI time series in the dLPFC and dACC during this task. Our approach for measuring the correlation is similar to the beta-series approach used by Rissman et al (37) and meant to optimize the measurement of correlations in different phases of a multi-phase task, (e.g., in this case the preparation versus decision phase of the POP task). We deviated from the beta-series approach in two ways: 1. Rather than comparing the correlation of time series on the same trial, we compared dACC activity during the decision phase of a given trial with the left BA46 activity on the subsequent trial. This approach was chosen because models of cognitive-control associated with tasks such as the POP task (38) suggest that conflict on one trial (high dACC during decision phase) should lead to high dLPFC preparatory load on the next trial. 2. Rather than generating the individual trial measures (i.e., betas) using multiple regression equations, we used the peak percent signal change during each trial phase. This is a similar, though simpler method, as it is not dependent on estimating the individual subject's HRF. Also the percent signal measure is particularly meaningful in our studies as it is the same measure we plot and use in our regional time-series analyses. As in the beta-series approach the series of individual trial phase measurements was then correlated

across regions. The correlation coefficients for each participant were then Z-transformed (using the Fisher-Z transformation) for inter-individual comparisons.

Results

Behavioral Performance and Treatment Response

The RTs and accuracy for the comparison group and the patients are shown in Figure 2. For 4 of the participants (2 elderly non-depressed, 1 patient pre-treatment, and 1 patient post-treatment), the behavioral data were incomplete due to computer errors, and thus these individuals were excluded from this analysis. When data from participants at baseline (patients pre-treatment and non-depressed comparison participants) were combined, the behavioral data reflected the expected load-effect (longer latency and lower accuracy for high-load versus low-load trials) for both RT ($t(21)=4.46$, $p=.0001$) and accuracy ($t(21)=2.57$, $p=.018$). The RT load-effect across groups were not significantly different: high-load RT - low-load RT, patients versus non-depressed comparison participants $t(21)=1.55$, $p=0.14$; pre- versus post-treatment depressed patients $t(12) = -1.16$, $p = 0.27$ (by matched pair t-test); and non-depressed comparison participants versus post-treatment patients $t(21)=.19$, $p=.85$. However, with respect to accuracy, there was a significant difference in performance, with the post-treatment patients showing a significantly increased load-effect relative to non-depressed comparison participants $t(21)=2.23$, $p=.035$. The other two comparisons of accuracy were not significant. The difference in the accuracy load-effect may indicate that the depressed participants were less vigilant on their return visit. However, this interpretation is speculative. Nevertheless, because the error trials were excluded from the fMRI analysis, this group difference in performance did not affect the fMRI signal data. Within-group paired t-tests comparing RT and accuracy during the early (first 20 trials) and later (last 20 trials) portions of the task, did not show any significant differences for these behavioral performance measures. This lack of significance in performance on the early versus late trials suggests that fatigue is not a significant factor in performance. However, it is possible that fatigue and learning occured, and that their possibly opposing effects canceled each other with respect to performance.

All 13 depressed participants showed a marked decrease in their score on the HRSD, mean pre-treatment HRSD=19.7 (SD=4.2) and post-treatment HRSD=7.5 (SD=4.8).

Mean Time-Series

The identified ROIs for each participant were used to generate a mean time-series associated with each condition (high-load or low-load, e.g., Figure 3). The trials were averaged within each condition, and thus the time course graph shows the signal across the different scan numbers (1-10). Since 10 scans were acquired over the course of each trial the graph shows the average course (per condition) across these 10 scans (20 seconds). The mean signal on high-load and low-load trial types were then compared within and between groups (Table II, Figure 4). As expected, when all participants at baseline were pooled (depressed pre-treatment and comparison subjects), the high-load trials were associated with a significantly higher activation peak in all dLPFC ROIs. Also as seen in the table (in t-tests comparing the patients pre- and post-treatment with elderly comparison participants), the elderly comparison participants (abbreviated to EC here on) showed a significantly greater peak activation than the LLD patients before treatment in left BA46. After treatment, although the dLPFC showed persistent decreased activation in the left BA46, (relative to EC participants) there appears to be increased activation in right BA46 and right BA9, on the high-load trials (Figures 3 & 4). To test whether this difference in the high-load trials was significant, we performed a matched-pairs t-test comparing the activity on the high-load trials pre- versus post-treatment on scans 2-5. On scan 5 in right BA46 we found a significant increase in the post-treatment activity

relative to pre-treatment ($t(25)=2.17$, $p<.02$). The one-tailed significance is reported since we hypothesized increased activation post-treatment relative to pre-treatment.

A similar pattern was found in the dACC. In this case, none of the group differences were statistically significant, but the pattern of activation changes followed that seen in the dLPFC. Overall, there was lower activation when elderly participants were evaluated as been depressed, which ameliorated with treatment (and response).

Whole Brain Voxel-Wise Analysis

In addition to the ROI-based analysis, an exploratory whole brain voxel-wise analysis was also done. The results of this analysis (illustrated in Figure 5) are qualitatively similar to the pattern seen in the ROI-based analysis. For the main effect of scan number (i.e., the main effect of task) mid-line dorsal ACC activation was found in all three groups. Significant left dLPFC activation was found in the EC and in depressed patients after treatment, but was not found in the patients before treatment.

Functional Connectivity

The results of the connectivity correlation analysis are shown in Table III and Figure 6. As can be seen in the figure, both EC and patients groups showed the predicted positive correlation between dACC and dLPFC activity on the subsequent trial. As predicted, there was a significantly lower correlation in the LLD patients pre-treatment versus EC participants; in right BA46, $t(24)=2.48$, $p=.01$ (one-tailed), suggesting decreased functional connectivity. An important question is whether the altered functional connectivity between the dACC and dLPFC regions resolves with treatment. As shown in Figure 6, the normalized correlation measure for right BA46 did not significantly differ in the pre- and post-treatment time periods ($t(24)=0.8$, $p=0.2$). Thus, unlike in the regional time-series analysis in the dACC, there did not appear to be a resolution of the altered connectivity after treatment for LLD. However, there was a significant increase in pre- to post-treatment correlation measures for a different region, left BA9 ($t(24) = 2.19$, $p<.02$, one-tailed). This region, however, showed only a statistical trend of lower correlation in patients pre-treatment relative to EC participants ($t(24)=1.64$, $p < .06$, one-tailed. Thus, it remains unclear whether the change in this region truly reflects a resolution of altered connectivity.

Estimated Movement Data

Movement correction was performed using a 6-parameter rigid body linear algorithm (23). None of the participants (EC or depressed) had greater than 2mm or 2 degrees of incremental movement on any parameter. None of the parameters differed significantly across groups. Thus, it is unlikely that group differences in movement affected our results.

Discussion

This study contrasted the BOLD fMRI signal in LLD and elderly comparison participants while they performed a cognitive-control task. Our primary aim was to investigate prefrontal function to test the frontostriatal dysfunction hypothesis of LLD. As predicted, we found significant differences in both prefrontal activation and functional connectivity in depressed versus comparison participants both before and after treatment.

Functional neuroimaging studies comparing elderly people with and without depression are potentially confounded by differences in neuroanatomy between groups, which can lead to more alignment error in depressed individuals versus otherwise healthy comparison groups. In the current study, we addressed this potential issue by using a single-subject ROI-based

analysis. This approach limits errors due to poor registration by selecting the ROI separately for each individual, using a non-linear warp in native anatomic space.

Given this study design and the small number of participants it is difficult to determine whether the change is due to remission of depression or whether the change is secondary to the specific treatment effect (i.e., the pharmacodynamic effect of paroxetine). Another possibility is that paroxetine (through activity on the cerebrovasculature) could have affected the underlying coupling of neural activity to the BOLD response. In particular, it is known that serotonin is involved in cerebrovascular regulation, and thus it is possible that selective serotonin reuptake inhibitors (such as paroxetine) could influence the BOLD signal even without influencing neural activity. Since in the current study we found regionally specific BOLD effects, we believe it is unlikely that paroxetine's effect on the BOLD response accounted for the current results.

A primary motivation of this study was to investigate the relation of LLD to prefrontal function. We hypothesized that consistent with the frontostriatal hypothesis of LLD there would be significant differences in these regions while performing cognitive tasks that engage those regions, and that some, but not all, of the observed changes would resolve with treatment; thus suggesting both episodic and persistent neurobiologic changes in LLD. We found evidence supporting this model. Both regional prefrontal fMRI activity and functional connectivity were decreased during a LLD episode and some of these changes appeared to resolve with treatment. These findings support a model that some of the regional activation changes (especially the dLPFC) are episodic, which are especially responsive to treatment. However, other effects, such as the functional connectivity, may be persistent, related to structural brain changes. These persistent effects may underlie the continued vulnerability of LLD patients for recurrent depressive episodes.

Acknowledgments

This research was supported by AAGP Pfizer/Eisai Fellowship (HJA), Hartford AFAR Fellowship (HJA), NARSAD, Pittsburgh Foundation, and NIMH grants T32-MH19986, R25-MH060473, K02-MH064190, K23-MH64678, K01-MH01684, R01-MH37869, R01-MH043832, R01- MH072947 and P30-MH52247. We thank Kate Fissell and the Clinical Cognitive Neuroscience laboratory at the University of Pittsburgh for their assistance.

References

1. Beekman AT, Copeland JR, Prince MJ. Review of community prevalence of depression in later life. Br J Psychiatry 1999;174:307–311. [PubMed: 10533549]
2. Murray, CJL.; Lopez, AD.; Harvard School of Public Health. et al. The global burden of disease: a comprehensive assessment of mortality and disability from diseases, injuries, and risk factors in 1990 and projected to 2020. Published by the Harvard School of Public Health; Cambridge, MA: 1996. on behalf of the World Health Organization and the World Bank; Distributed by Harvard University Press
3. Frasure-Smith N, Lesperance F, Talajic M. Depression following myocardial infarction. Impact on 6-month survival. Jama 1993;270:1819–1825. [PubMed: 8411525]
4. Schulz R, Beach SR, Ives DG, et al. Association between depression and mortality in older adults: the Cardiovascular Health Study. Archives of Internal Medicine 1761;160:1761–1768. [PubMed: 10871968]see comment
5. Conwell Y, Duberstein PR, Cox C, et al. Relationships of age and axis I diagnoses in victims of completed suicide: a psychological autopsy study. Am J Psychiatry 1996;153:1001–1008. [PubMed: 8678167]
6. Administration on Aging. A Profile of Older Americans: 2003. U.S. Department of Health and Human Services; Washington, D.C.: 2003.
7. Lebowitz BD, Pearson JL, Schneider LS, et al. Diagnosis and treatment of depression in late life. Consensus statement update. Jama 1997;278:1186–1190. [PubMed: 9326481]

8. Alexopoulos GS, Kiosses DN, Klimstra S, et al. Clinical presentation of the “depression-executive dysfunction syndrome” of late life. Am J Geriatr Psychiatry 2002;10:98–106. [PubMed: 11790640]
9. Alexopoulos GS, Kiosses DN, Choi SJ, et al. Frontal white matter microstructure and treatment response of late-life depression: a preliminary study. Am J Psychiatry 2002;159:1929–1932. [PubMed: 12411231]
10. Hickie I, Scott E, Wilhelm K, et al. Subcortical hyperintensities on magnetic resonance imaging in patients with severe depression--a longitudinal evaluation. Biol Psychiatry 1997;42:367–374. [PubMed: 9276077]
11. Krishnan KR, Hays JC, Blazer DG. MRI-defined vascular depression. Am J Psychiatry 1997;154:497–501. [PubMed: 9090336]
12. Kumar A, Thomas A, Lavretsky H, et al. Frontal white matter biochemical abnormalities in late-life major depression detected with proton magnetic resonance spectroscopy. Am J Psychiatry 2002;159:630–636. [PubMed: 11925302]
13. Taylor WD, Hsu E, Krishnan KR, et al. Diffusion tensor imaging: background, potential, and utility in psychiatric research. Biol Psychiatry 2004;55:201–207. [PubMed: 14744459]
14. Butters MA, Whyte EM, Nebes RD, et al. The nature and determinants of neuropsychological functioning in late-life depression. Arch Gen Psychiatry 2004;61:587–595. [PubMed: 15184238]
15. Nobler MS, Mann JJ, Sackeim HA. Serotonin, cerebral blood flow, and cerebral metabolic rate in geriatric major depression and normal aging. Brain Res Brain Res Rev 1999;30:250–263. [PubMed: 10567727]
16. Aizenstein HJ, Butters MA, Clark KA, et al. Prefrontal and striatal activation in elderly subjects during concurrent implicit and explicit sequence learning. Neurobiol Aging 2006;27:741–751. [PubMed: 15935517]
17. Fitzgerald PB, Laird AR, Maller J, et al. A meta-analytic study of changes in brain activation in depression. Hum Brain Mapp. 2007
18. MacDonald AW 3rd, Cohen JD, Stenger VA, et al. Dissociating the role of the dorsolateral prefrontal and anterior cingulate cortex in cognitive control. Science 2000;288:1835–1838. [PubMed: 10846167]
19. Mayberg HS. Limbic-cortical dysregulation: a proposed model of depression. J Neuropsychiatry Clin Neurosci 1997;9:471–481. [PubMed: 9276848]
20. Beekman AT, de Beurs E, van Balkom AJ, et al. Anxiety and depression in later life: Co-occurrence and communality of risk factors. Am J Psychiatry 2000;157:89–95. [PubMed: 10618018]
21. Reynolds CF 3rd, Dew MA, Pollock BG, et al. Maintenance treatment of major depression in old age. N Engl J Med 2006;354:1130–1138. [PubMed: 16540613]
22. Folstein MF, Folstein SE, McHugh PR. “Mini-mental state”. A practical method for grading the cognitive state of patients for the clinician. J Psychiatr Res 1975;12:189–198. [PubMed: 1202204]
23. Woods RP, Grafton ST, Holmes CJ, et al. Automated image registration: I. General methods and intrasubject, intramodality validation. J Comput Assist Tomogr 1998;22:139–152. [PubMed: 9448779]
24. Rosano C, Aizenstein H, Cochran J, et al. Functional neuroimaging indicators of successful executive control in the oldest old. Neuroimage 2005;28:881–889. [PubMed: 16226041]
25. Rosano C, Aizenstein HJ, Cochran JL, et al. Event-related functional magnetic resonance imaging investigation of executive control in very old individuals with mild cognitive impairment. Biol Psychiatry 2005;57:761–767. [PubMed: 15820233]
26. Tzourio-Mazoyer N, Landeau B, Papathanassiou D, et al. Automated anatomical labeling of activations in SPM using a macroscopic anatomical parcellation of the MNI MRI single-subject brain. Neuroimage 2002;15:273–289. [PubMed: 11771995]
27. Carter CS, Macdonald AM, Botvinick M, et al. Parsing executive processes: strategic vs. evaluative functions of the anterior cingulate cortex. Proc Natl Acad Sci U S A 2000;97:1944–1948. [PubMed: 10677559]
28. Wu M, Carmichael O, Lopez-Garcia P, et al. Quantitative comparison of AIR, SPM, and the fully deformable model for atlas-based segmentation of functional and structural MR images. Hum Brain Mapp 2006;27:747–754. [PubMed: 16463385]

29. Yoo, T. Insight into Images: Principles and Practice for Segmentation, Registration, and Image Analysis. AK Peters Ltd.; Wellesey, MA: 2004.

30. Zhang Y, Brady M, Smith S. Segmentation of brain MR images through a hidden Markov random field model and the expectation maximization algorithm. IEEE Transaction of Medical Imaging 2001;20:45–57.

31. Huettel SA, Singerman JD, McCarthy G. The effects of aging upon the hemodynamic response measured by functional MRI. Neuroimage 2001;13:161–175. [PubMed: 11133319]

32. D'Esposito M, Zarahn E, Aguirre GK, et al. The effect of normal aging on the coupling of neural activity to the bold hemodynamic response. Neuroimage 1999;10:6–14. [PubMed: 10385577]

33. Aizenstein HJ, Clark KA, Butters MA, et al. The BOLD hemodynamic response in healthy aging. Journal of Cognitive Neuroscience 2004;16:786–793. [PubMed: 15200706]

34. Friston KJ, Holmes AP, Worsley KJ, et al. Statistical parametric maps in functional imaging: A general linear approach. Human Brain Mapping 1994;2:189–210.

35. Fissell K, Tseytlin E, Cunningham D, et al. Fiswidgets: a graphical computing environment for neuroimaging analysis. Neuroinformatics 2003;1:111–125. [PubMed: 15055396]

36. Forman SD, Cohen JD, Fitzgerald M, et al. Improved assessment of significant activation in functional magnetic resonance imaging (fMRI): use of a cluster-size threshold. Magn Reson Med 1995;33:636–647. [PubMed: 7596267]

37. Rissman J, Gazzaley A, D'Esposito M. Measuring functional connectivity during distinct stages of a cognitive task. Neuroimage 2004;23:752–763. [PubMed: 15488425]

38. Kerns JG, Cohen JD, MacDonald AW 3rd, et al. Anterior cingulate conflict monitoring and adjustments in control. Science 2004;303:1023–1026. [PubMed: 14963333]

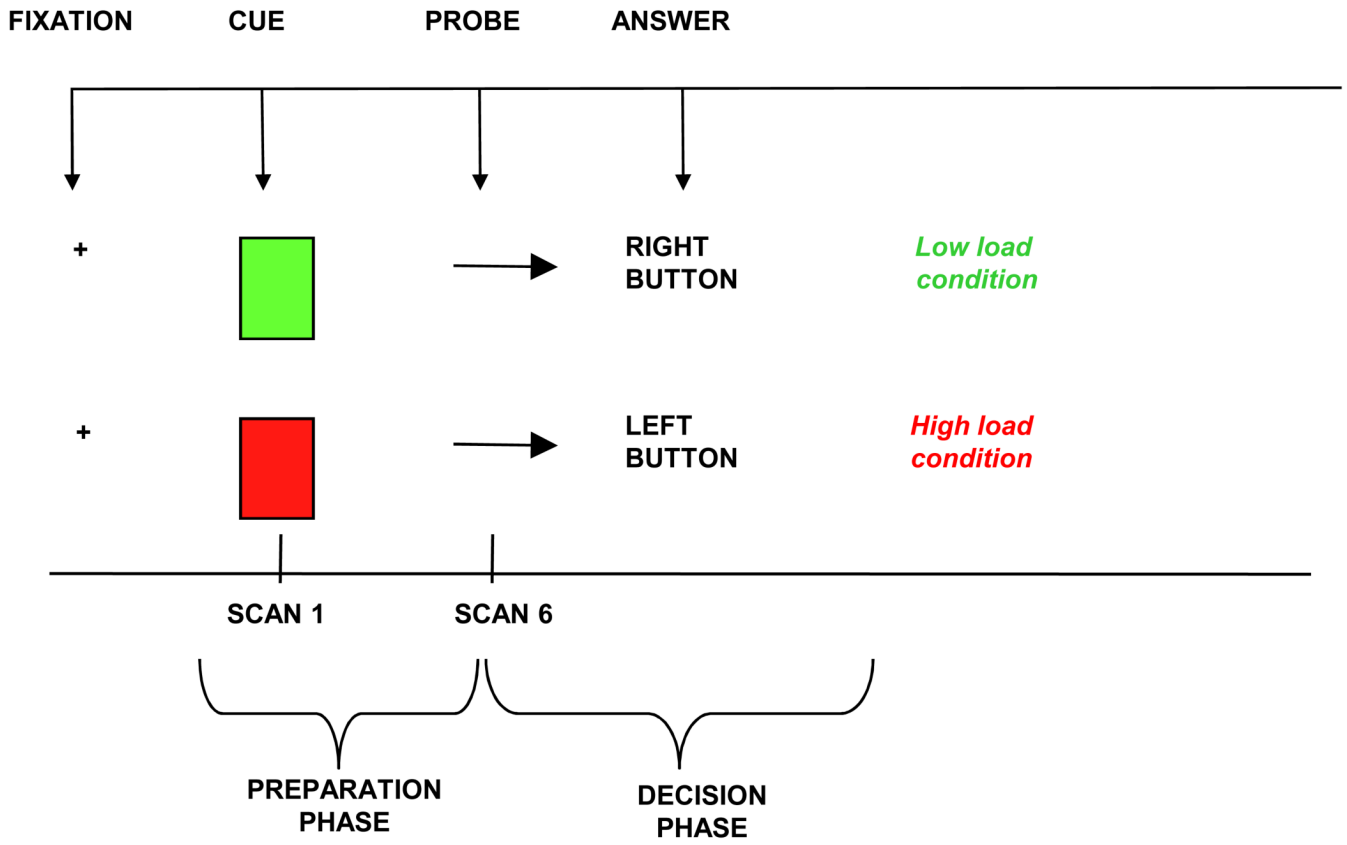

Figure 1.
Individual trial of the POP task. Red or Green square is followed, after a 10-second delay, by an arrow pointing to the right or the left.

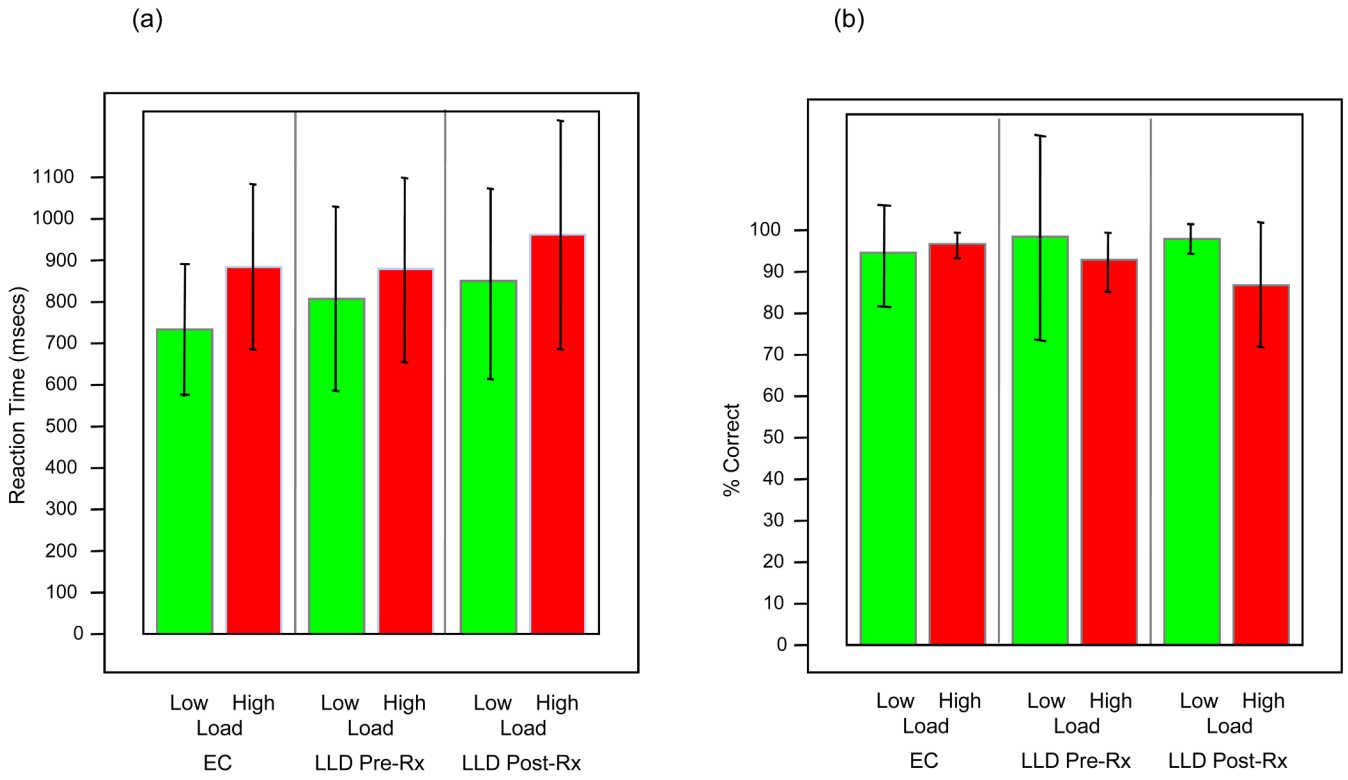

Figure 2.
Behavioral results during the fMRI scanning, reaction time (a) and accuracy (b). Error bars represent +/- 1 standard deviation of the mean.

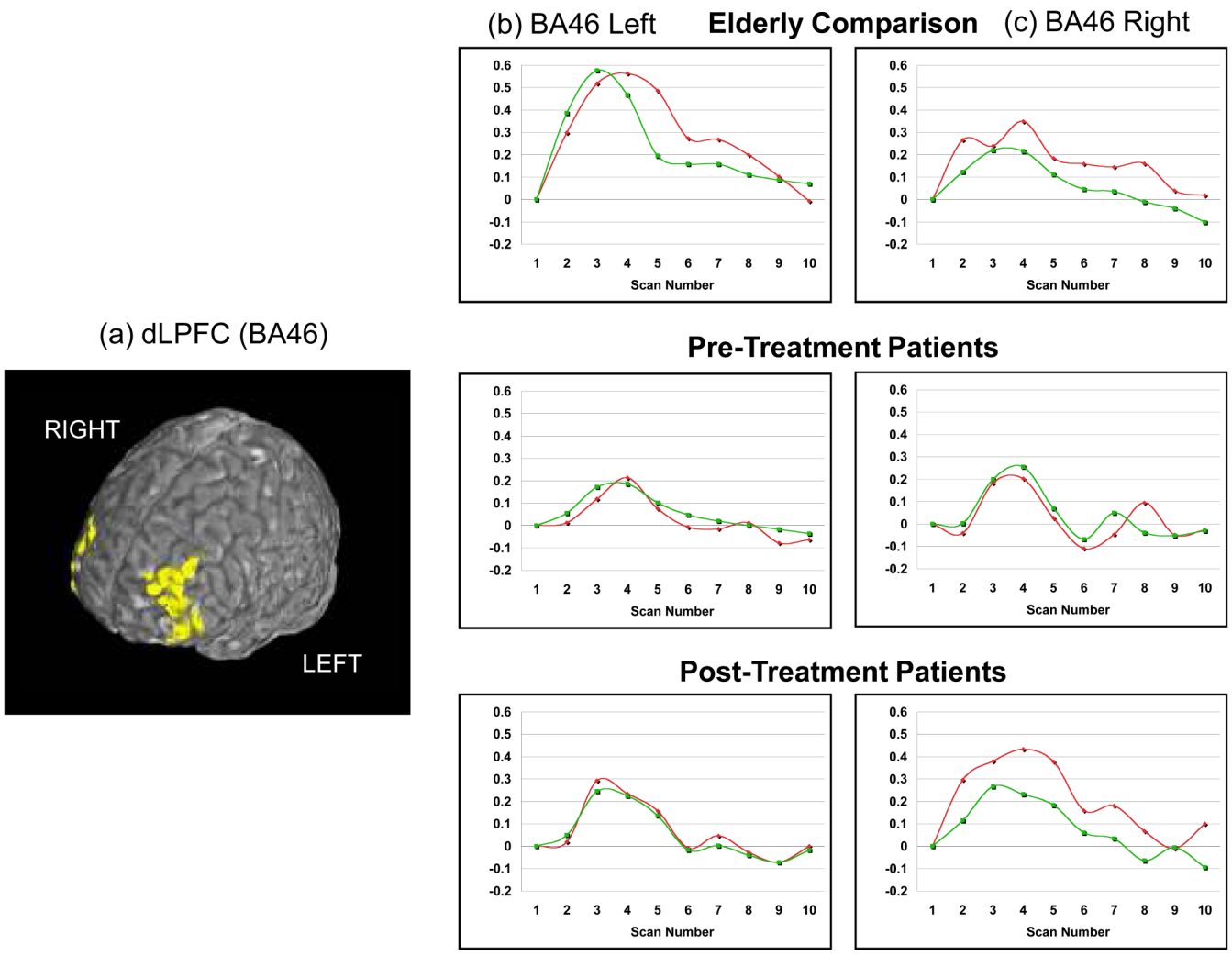

Figure 3.
Time-series for fMRI activation in the dLPFC (BA46). The regions of interest (a) are displayed on the reference□brain, and percent signal change over the course of a trial are shown □for both right BA46 (b) and left BA46 (c).□□

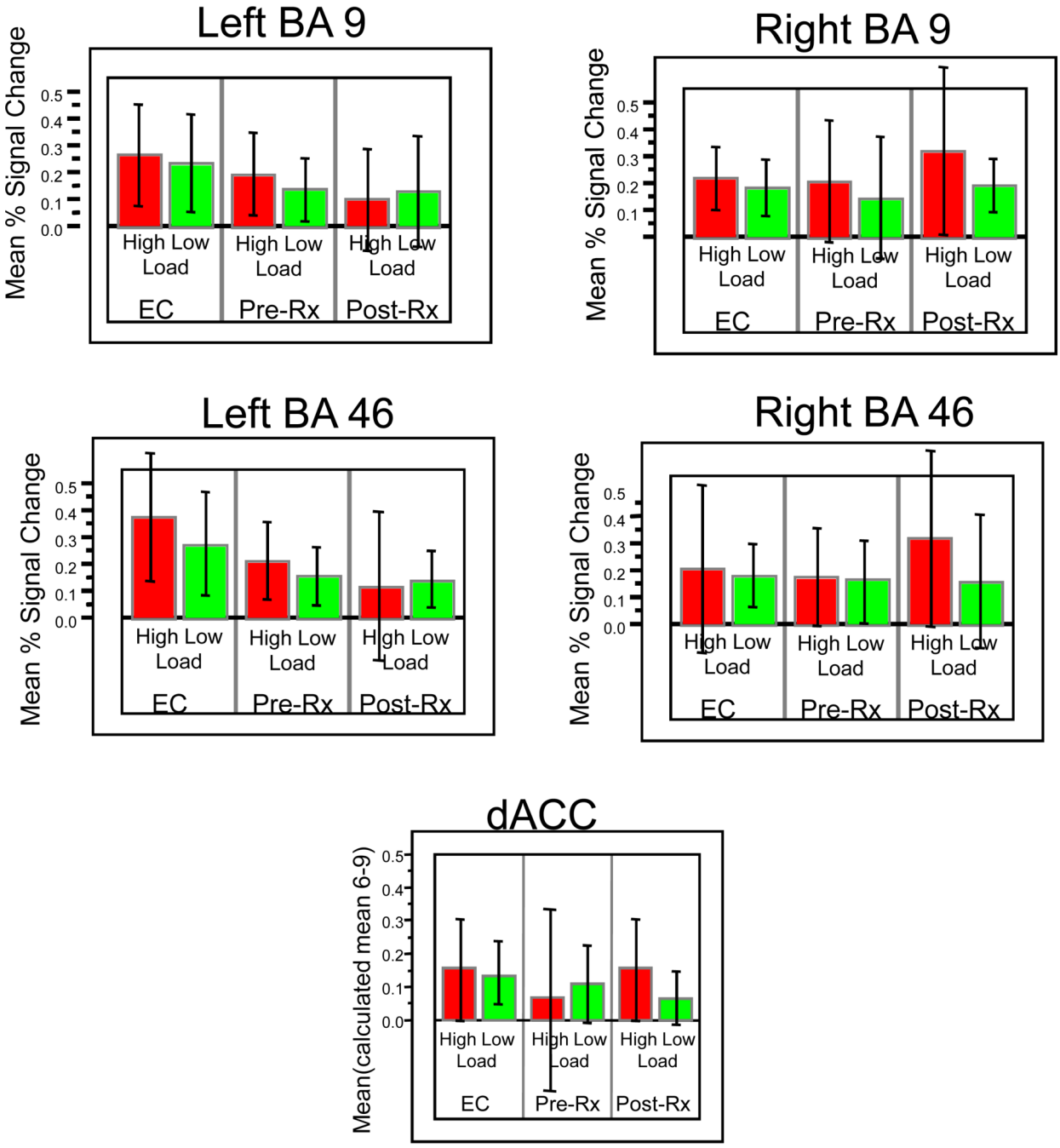

Figure 4.
Mean percent signal change on high-load and low-load trials shown for the 5 ROIs. Error bars represent +/- 1 standard deviation of the mean.

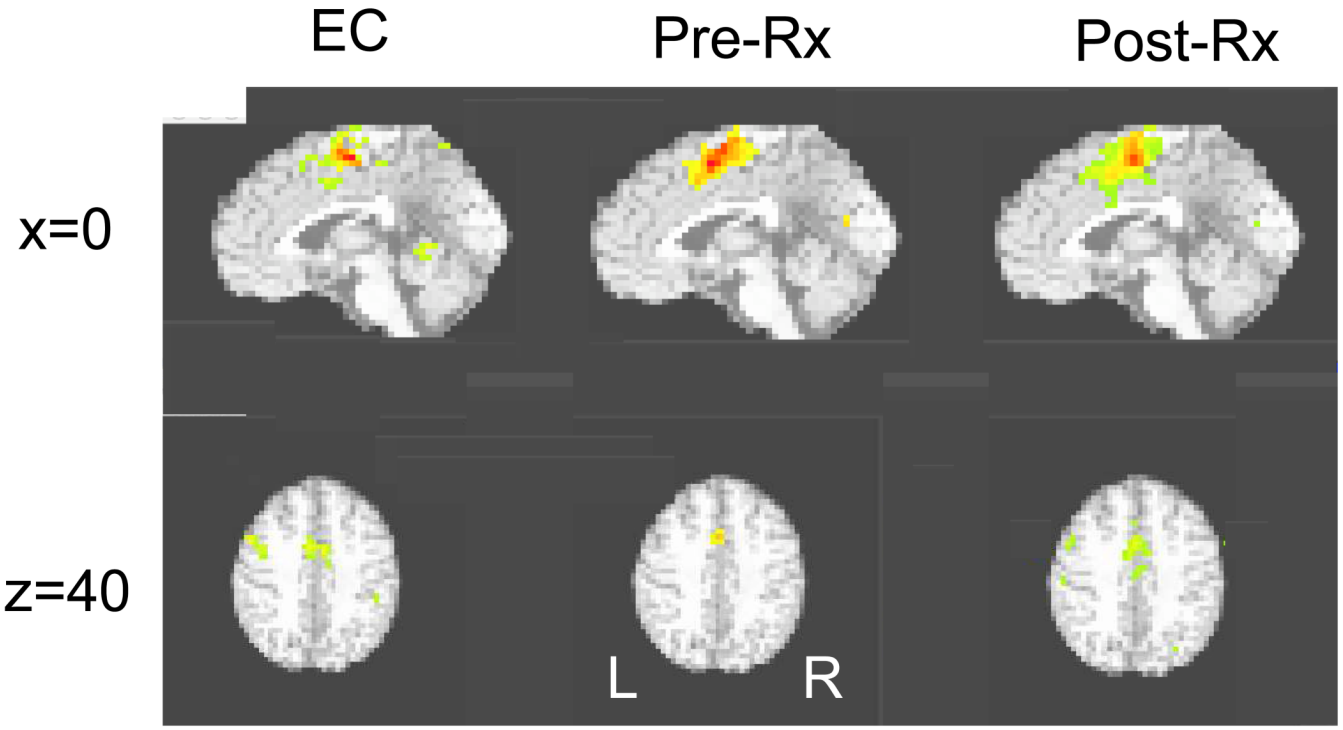

Figure 5.
Mean normalized correlation coefficients of time series in Elderly Comparison Participants (EC), LLD pre-treatment (Pre-Rx), and LLD post-treatment (Post-Rx) between dACC and BA46 right. Correlations were performed on the extracted fMRI time-series, comparing the peak at dACC during the decision phase of a trial with the peak in left BA46 during the cue phase of the next trial, thus estimating the trial-to-trial PFC adjustment based on ACC conflict. Error bars represent +/- 1 standard deviation of the mean.

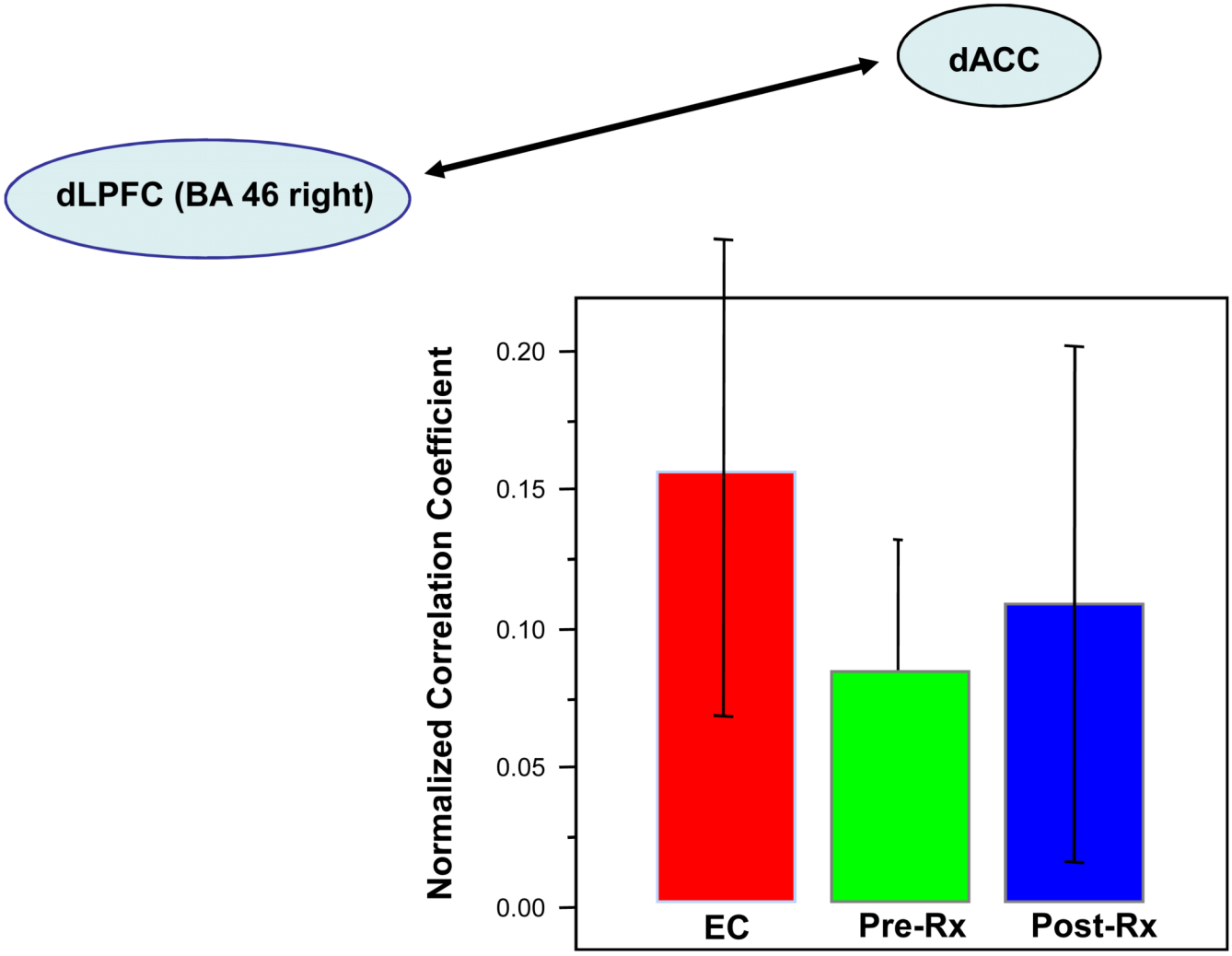

Figure 6.
Mean normalized correlation coefficients of timeseries in Elderly Comparison Participants (EC), LLD pre-treatment (Pre-Rx), and LLD post-treatment (Post-Rx) between dACC and BA46 right. Correlations were performed on the extracted fMRI time-series, comparing the peak at dACC during the decision phase of a trial with the peak in left BA46 during the cue phase of the next trial, thus estimating the trial-to-trial PFC adjustment based on ACC conflict. Error bars represent +/- 1 standard deviation of the mean.

Table I

Demographics

	Elderly Comparison	Depressed Pre-Treatment	Depressed Post-Treatment
N	13	13	13
Age (yrs)	68.8 +/- 5.79	69.1 +/- 5.50	69.2 +/- 5.41
Gender	6M, 7F	6M, 7F	6M, 7F
Education (yrs)	15.8 +/- 2.91	14.1 +/- 2.81	
Race	11C, 2AA	12C, 1AA	12C, 1AA
Mini-Mental Status Exam	29.0 +/- 1.41	27.8 +/- 3.42	28.5 +/- 1.71
Hamilton Rating Scale	1.3 +/- 1.65	19.7 +/- 4.25	7.5 +/- 4.82
MATTIS Dementia Rating Scale	141.3 +/- 1.49	138.6 +/- 5.27	137.5 +/- 7.17
Age of Depression Onset	N/A	63.8 +/- 9.19	

Table II

Regional BOLD Signal Change

		Red vs Green Trials, across all participants t(25), p	EC vs. Pre-Treatment t(25), p	Post- vs. Pre-Treatment t(12)*, p	EC vs. Post-Treatment T(25), p
BA 46	L	**2.57, .016**	**1.9, .035**	-1.15, .86	**2.36, .013**
	R	1.94, .064	.27, .40	1.11, .14	-.81, .85
BA 9	L	**2.22, .036**	.82, 0.15	-1.13, .86	**1.93, .03**
	R	**3.08, .005**	.19, .42	1.17, .13	-.89, .77
dACC	M	1.74, .095	1.58, .06	1.41, .09	50, .31

Note. EC, Elderly comparison.

* paired T test

Table III

Functional Connectivity: dLPFC sub-region to dACC

		EC vs. Pre-Treatment t(24), p	Post- vs. Pre-Treatment t(12)*, p	EC vs. Post-Treatment t(24), p
BA46	Left	**1.77, 0.04**	1.45, 0.09	0.53, 0.30
	Right	**2.48, 0.01**	0.68, 0.25	1.3, 0.10
BA09	Left	1.64, 0.06	**2.19, 0.02**	0.63, 0.27
	Right	0.83, 0.21	0.60, 0.28	0.36, 0.36

Note. EC, Elderly control.

* paired T test